Anisotropic flows in reggeon theory

K. G. Boreskov[a][*], A. B. Kaidalov[a][†], O. V. Kancheli[a][‡]

[a] *Institute of Theoretical and Experimental Physics*

B. Cheremushkinskaya 25, Moscow, 117218 Russia

Abstract

We analyze azimuthal anisotropy in heavy ion collisions related to the reaction plane in terms of standard reggeon approach and find that it is nonzero even when the final state interaction is switched off. This effect can be interpreted in terms of partonic structure of colliding nuclei. We use Feynman diagrams analysis to describe details of this mechanism. Main qualitative features of the appropriate azimuthal correlations are discussed.

Investigations of azimuthal anisotropy of secondary particle distributions in heavy ions collisions is used as an effective tool for analysis of dynamical mechanisms of these processes. Anisotropic flows and, in particular, elliptic flow $v_2 \equiv \langle \cos 2\phi \rangle$ are considered usually as an important source of information about properties of a dense state of hadronic matter formed in the anisotropic overlap region of colliding nuclei (see e.g. [2] - [9]).

Crucial point is the relation of the anisotropy to the reaction plane orientation (azimuthal correlations not related to this orientation are called non-flow correlations). The dependencies of flow coefficients on c.o.m. energy, centrality, rapidity range and transverse momentum of secondaries are ascribed usually to anisotropic properties of strongly interacting matter at early times after collision. It is assumed that anisotropic flows are due to final state interactions and in hydrodynamic models originate from pressure gradients connected to original asymmetry in the configuration space for noncentral collisions. Practically all existing models for anisotropic flows use classical description of processes.

We use quantum relativistic approach, based on analysis of Feynman diagrams and reggeon theory for a study of anisotropic flows in collisions of hadrons and nuclei at high energies. We will show that a part of azimuthal anisotropy can be related to properties of *initial* state of a fast nucleus. Namely, we analyze azimuthal correlations present in partonic configurations of fast colliding nuclei. Thus a part of the observed azimuthal asymmetry of final particles can come from parton correlations in initial state. We shall demonstrate how anisotropic flows in this case are related to the anisotropy of the overlap region.

The simplest way to study such phenomena theoretically is to use the reggeon diagrams for inclusive cross sections, where all details of parton interactions are encoded in vertices and Regge trajectories.

A simplest way to produce secondary particles at high energy is given by multiperipheral diagram of Fig.1a. Inclusive cross section is described by the reggeon diagram of Fig.1b which corresponds to squared multiparticle amplitude with fixed momentum p of a single detected particle.

Single particle inclusive cross section is related to the amplitude $G(\mathbf{q}, \mathbf{p})$ of the diagram of Fig.1b at zero transfer momentum $\mathbf{q} = 0$:

$$F_{incl}(\mathbf{p}_t; y) \equiv \frac{d\sigma}{d^2\mathbf{p}_t dy} \propto G(\mathbf{q} = 0; \mathbf{p}_t, y) \ , \tag{1}$$

[*]**e-mail**: boreskov@itep.ru

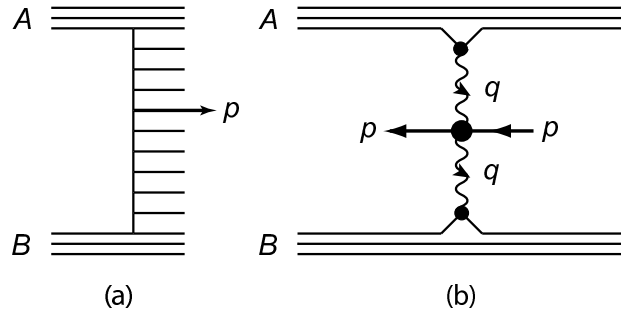[†]**e-mail**: kaidalov@itep.ru

[‡]**e-mail**: kancheli@itep.ru

Figure 1: Reggeon diagram for one-particle inclusive production

where p_t and y are transverse momentum and rapidity of the registered particle. We, however, need to calculate a contribution of this diagram at various values of $\mathbf{q}$ in order to find a correlation between transverse momentum $\mathbf{p}_t$ and impact parameter value for colliding nuclei, $\mathbf{b}$. This relation is given by Fourier transform of $G(\mathbf{q}; \mathbf{p}_t, y)$

$$\widetilde{F}_{incl}(\mathbf{p}_t, y; \mathbf{b}) \sim \widetilde{G}(\mathbf{b}; \mathbf{p}_t, y) = \int \frac{d^2\mathbf{q}}{(2\pi)^2} \ e^{i\mathbf{b}\mathbf{q}} \ G(\mathbf{q}; \mathbf{p}_t, y) \ . \tag{2}$$

Here

$$G(\mathbf{q}; \mathbf{p}_t, y) = F_A(q)D(\mathbf{q}; y)\gamma(\mathbf{q}, \mathbf{p}_t)D(\mathbf{q}; Y - y)F_B(q) \ , \tag{3}$$

where $F_{A,B}$ are 2-dimensional form factors of colliding nuclei which are Fourier transforms of their 2-dimensional profiles, $T_{A,B}(b)$,

$$F_{A,B}(q) = \int d^2b \ e^{-i\mathbf{q}\mathbf{b}}T_{A,B}(b) \ , \qquad F_A(0) = A, \quad F_B(0) = B, \tag{4}$$

and functions $D(\mathbf{q}; y), D(\mathbf{q}; Y - y)$ are connected to s-channel discontinuities of reggeon amplitudes ("cut reggeons").

We use an exponential parameterization of reggeon vertex $g_N \exp(-R_0^2\mathbf{q}^2)$ and linear Regge trajectory $\alpha(\mathbf{q}^2) = \alpha(0) - \alpha'\mathbf{q}^2$.

$$D(\mathbf{q}; y) \equiv 2 \operatorname{Im} f(\mathbf{q}; y) = g_N e^{-(R_0^2 + \alpha'y)q^2} e^{[\alpha(0)-1]y} \ . \tag{5}$$

An inclusive vertex of the reggeon diagram $\gamma(\mathbf{q}, \mathbf{p}_t)$ depends on 2-dimensional momenta $\mathbf{p}_t$ and $\mathbf{q}$. For estimates we will use the phenomenological parametrization

$$\gamma(\mathbf{q}, \mathbf{p}_t) = \gamma_0 \exp\{-r_q^2\mathbf{q}^2 - r_p^2\mathbf{p}_t^2 - \epsilon r_0^4(\mathbf{p}_t\mathbf{q})^2\} \ . \tag{6}$$

Here dimensional coefficients r_q, r_p are expected to be of typical hadronic sizes about $r_0 = 1$ fm, and ϵ of order of 1.

The dependence on variable $(\mathbf{p}_t\mathbf{q})$ is crucial for appearance of azimuthal correlations typical for elliptic flow. Note that the terms proportional to the odd powers of $\mathbf{p}_t\mathbf{q}$ should be absent if both reggeons have positive C-parity (like pomerons) because the vertex should be even under the change $\mathbf{p}_t \to -\mathbf{p}_t$. More detailed analysis of structure and value of the vertex $\gamma(\mathbf{q}, \mathbf{p}_t)$ will be performed below.

The elliptic flow v_2 is defined as a second Fourier coefficient in an azimuthal dependence of inclusive spectrum

$$\frac{d\sigma}{dp_t^2 d\phi} \propto 1 + \sum_1^\infty 2v_n(b; p_t, y) \cos(n\phi) \ , \tag{7}$$

2

where ϕ is an azimuthal angle between impact parameter $\mathbf{b}$ which determines the reaction plane and transverse momentum $\mathbf{p}_t$. Thus,

$$v_2(b; p_t, y) \equiv \frac{C_2}{C_0} = \frac{\int d\phi \; \cos(2\phi) \; G(\mathbf{b}; \mathbf{p}_t, y)}{\int d\phi \; G(\mathbf{b}; \mathbf{p}_t, y)} \; . \tag{8}$$

For the vertex function parameterized by eq.(6) one gets

$$C_n(b; p_t, y) = \int q dq J_n(bq) F_A(q^2) F_B(q^2) D(q; y) D(q, Y - y) c_n(q; b, p_t) , \quad n = 0, 2, \tag{9}$$

with

$$C_0(q; b, p_t) = I_0(\epsilon r_0^4 p_t^2 q^2 / 2) \; e^{-\epsilon r_0^4 p_t^2 q^2 / 2} \; , \tag{10}$$

$$C_2(q; b, p_t) = I_1(\epsilon r_0^4 p_t^2 q^2 / 2) \; e^{-\epsilon r_0^4 p_t^2 q^2 / 2} \; .$$

where I_0, I_1 are the standard Bessel functions.

To estimate an order of the effect let us first make the calculation with the approximate Gaussian parameterization of nuclear form factors $F_{A,B}(q^2)$:

$$F_{A,B}(q^2) = \exp(-R_{A,B}^2 q^2 / 4) \; . \tag{11}$$

Then

$$v_2(b; p_t, y) = \frac{I_1(\alpha/2)}{I_0(\alpha/2)} \tag{12}$$

with

$$\alpha = \frac{\epsilon r_0^4 p_t^2 b^2}{R^2(R^2 + 4\epsilon r_0^4 p_t^2)} \; , \qquad R^2 = R_A^2 + R_B^2 + R_{regge}^2(Y) \; . \tag{13}$$

For $\alpha \ll 1$ we have :

$$v_2 \simeq \frac{\alpha}{4} \simeq \epsilon \, (r_0 p_t)^2 \left(\frac{r_0}{R}\right)^2 \left(\frac{b}{2R}\right)^2 \; . \tag{14}$$

Thus, v_2 is proportional to the "ellipticity" ϵ of the inclusive vertex γ. The sign of v_2 is the same as the one of ϵ which can be both positive and negative depending on dynamical structure of the inclusive vertex (see discussion below). The formula (14) reveals an increase of the v_2 with transverse momentum $\mathbf{p}_t$ and impact parameter b.

Presentation of formulas in terms of impact parameters allows us to give more instructive interpretation of the results. Eqs.(2),(3) in these variables have the form:

$$G(\mathbf{b}; \mathbf{p}_t, y) \sim \int d^2\boldsymbol{\beta}_1 \int d^2\mathbf{b}_1 \int d^2\mathbf{b}_2 \int d^2\boldsymbol{\beta}_2 \; T_A(\boldsymbol{\beta}_1) \; t_1(\mathbf{b}_1 - \boldsymbol{\beta}_1; y)$$
$$\times \; \Gamma(\mathbf{b}_2 - \mathbf{b}_1, \mathbf{p}_t) \; t_2(\boldsymbol{\beta}_2 - \mathbf{b}_2; Y - y) \; T_B(\mathbf{b} - \boldsymbol{\beta}_2) \; . \tag{15}$$

Here $\boldsymbol{\beta}_1$ and $\mathbf{b} - \boldsymbol{\beta}_2$ are the positions of participant nucleons of the nuclei A and B with nuclear profiles T_A and T_B, $t(\boldsymbol{\beta}; y)$ is a Fourier transform of reggeon propagator $D(\mathbf{q}; y)$ and $\Gamma(\mathbf{b}; \mathbf{p}_t)$ is a Fourier transform of the inclusive vertex $\gamma(\mathbf{q}, \mathbf{p}_t)$:

$$\Gamma(\mathbf{b}; \mathbf{p}_t) = \int \frac{d^2\mathbf{q}}{(2\pi)^2} \; e^{i\mathbf{q}\mathbf{b}} \gamma(\mathbf{q}, \mathbf{p}_t) \; . \tag{16}$$

3

For the exponential model approximation (6), one has

$$\Gamma(\mathbf{b}; \mathbf{p}_t) = \frac{\pi e^{-r_p^2 p_t^2}}{\sqrt{r_q^2(r_q^2 + \epsilon r_0^4 p_t^2)}} \exp\left(-\frac{b_x^2}{4(r_q^2 + \epsilon r_0^4 p_t^2)} - \frac{b_y^2}{4r_q^2}\right) , \qquad (17)$$

where b_x is a component of $\mathbf{b}$ along $\mathbf{p}_t$ and b_y in the transverse direction.

In order to reveal a structure of Eq.(15) it can be written symbolically as a number of convolutions with symbolic notation $f \otimes g$ for convolution of functions f and g:

$$F_{incl}(\mathbf{p}_t, y; \mathbf{b}) \sim T_A \otimes t(y) \otimes \Gamma \otimes t(Y - y) \otimes T_B . \qquad (18)$$

Convolutions in eq.(15) can be done in arbitrary order, so it is equivalent to

$$F_{incl}(\mathbf{p}_t, y; \mathbf{b}) \sim T_{int} \otimes \Gamma = \int d^2\mathbf{a} T_{int}(\mathbf{b} - \mathbf{a})\Gamma(\mathbf{a}; p_t) . \qquad (19)$$

Here the function T_{int} which characterize a region of interaction of nuclei in $\mathbf{b}$ space is a convolution of the nuclear overlap $T_{AB} = T_A \otimes T_B$ and combined reggeon amplitude t_{regge}:

$$T_{int} = T_{AB} \otimes t_{regge} ,$$

where

$$t_{regge}(b; Y) = t(y) \otimes t(Y - y) = \frac{g_N^2}{4\pi R_{regge}^2(Y)} \exp\left(-\frac{b^2}{4R_{regge}^2(Y)}\right) ,$$
$$R_{regge}^2(Y) = 2R_0^2 + \alpha'Y ,$$

describes the regge-interaction amplitude of nucleons from colliding nuclei.

For Gaussian parameterization of nuclear profiles T_A, T_B all convolutions have the Gaussian form again, resulting in the same final answer (12).

In the impact parameter representation it is easy to see an origin of the correlation between directions of $\mathbf{b}$ and transverse momentum $\mathbf{p}_t$. Registration of the inclusive particle is realized by nonlocal probe which structure is determined by inclusive vertex $\Gamma(\mathbf{b}; \mathbf{p}_t)$. This vertex has an elliptic anisotropy in b-plane along the direction of $\mathbf{p}_t$. Due to this anisotropy the convolution of the overlap function T_{int} and Γ is sensitive to gradients of nuclear densities.

The size of the probe range is small in comparison to nuclear size $R_A \sim R_B \sim A^{1/3}r_0$, so it is possible to calculate the integral (19) expanding the smooth distribution $T_{int}(\mathbf{b} - \mathbf{a})$ over small corrections $a_x/R_A, a_y/R_A$. After integration over a_x, a_y we get explicitly anisotropic expression for the inclusive cross section (recall that the axis x is chosen along the momentum $\mathbf{p}_t$). Omitting higher order terms in a_i/R_A we have in approximation (6),(17)

$$F_{incl} \sim T_{int}(b^2) + 2(2r_q^2 + \epsilon r_0^4 p_t^2)\frac{dT_{int}(b^2)}{d(b^2)} + 4\frac{d^2 T_{int}(b^2)}{d(b^2)^2}\left[(r_q^2 + \epsilon r_0^4 p_t^2)b_x^2 + r_q b_y^2\right] , \qquad (20)$$

where derivatives are taken over the variable b^2. Thus, for the elliptic flow coefficient we have

$$v_2 \simeq \epsilon \frac{r_0^4 T_{int}''(b^2)}{T_{int}(\mathbf{b}^2)} \mathbf{p}_t^2 \mathbf{b}^2 . \qquad (21)$$

The second derivative of $T_{int}(\mathbf{b}^2)$ contains a small parameter of order of $(r_0/R_A)^4$ which appears explicitly in Eq.(14).

Let us stress that reggeon diagrams allow partonic interpretation which depends on chosen Lorentz frame. Reggeon exchanges are highly non-local in space-time due to their complicated multiparticle internal structure. From this viewpoint the fast hadron or nucleus is essentially

4

multiparton state of multiperipheral configuration (fig.1a represents the simplest example). The particles of such configuration are ordered in their rapidities and only most slow particles interact with a target. This means that in the lab frame related to the nucleus B the nucleus A is a multiparton state containing the detected particle with rapidity y and transverse momentum $\mathbf{p}_t$ among others. This state has already an anisotropy in partonic distributions due to correlation between parton transverse momentum $\mathbf{p}_t$ and its position $\mathbf{b}_1$ in impact parameter plane. If nuclear collision is central then the overlap region is isotropic and after integration over b_1 anisotropy disappears. At non-central collision, however, the overlap region has anisotropic almond shape and integration over this region keeps anisotropic distribution in $\mathbf{p}_t$.

The azimuthal partonic anisotropy can't be revealed with local probe which feels only partonic density. An information about density gradients and its higher derivatives can be obtained by means of nonlocal probes with typically hadronic range. Being restricted only with lower multipoles a structure of the probe can be written as

$$\Gamma(\mathbf{a};\mathbf{p}) \sim \left(1 + \bar{\delta}p_i\partial_i + (\beta\delta_{ij} + \bar{\epsilon}p_ip_j)\partial_i\partial_j + \dots\right)\delta^{(2)}(\mathbf{a}) , \tag{22}$$

where $\partial_i = \partial/\partial a_i$ and $\bar{\delta} \equiv \delta r_0^2$, $\bar{\epsilon} \equiv \epsilon r_0^4$ are dimensional coefficients of typical hadronic range. The first term measures parton density as well as the isotropic one with δ_{ij}, the second term feels gradients, and the ϵ-term gives an information about ellipticity of partonic distribution at the point of production of registered particle. So the distribution over transverse momenta turns out to be correlated with impact parameter $\mathbf{b}$:

$$\begin{aligned}
F_{incl}(\mathbf{p}_t;\mathbf{b}) &\sim T_{int} \otimes \Gamma = \int d^2\mathbf{a}\, T_{int}(\mathbf{b} - \mathbf{a})\Gamma(\mathbf{a};\mathbf{p}_t) \\
&\approx T_{int}(b^2) + \bar{\delta}p_{t\,i}\partial_i T_{int}(b^2) + \bar{\epsilon}p_{t\,i}p_{t\,j}\partial_i\partial_j T_{int}(b^2) \\
&\approx T_{int}(b^2) + 2\bar{\delta}(\mathbf{p}_t\mathbf{b})T'_{int}(b^2) + 4\bar{\epsilon}(\mathbf{p}_t\mathbf{b})^2 T''_{int}(b^2) ,
\end{aligned} \tag{23}$$

where T' denotes the derivative over b^2. This reproduces the elliptic flow coefficient $v_2 = \epsilon(\mathbf{p}_t\mathbf{b})^2 T''_{int}(b^2)$ (cf. with (21)). The δ-term corresponds to the first flow coefficient $v_1 = \delta(\mathbf{p}_t\mathbf{b})\,T'_{int}(b^2)$ (directed flow).

Let us estimate in simple models an anisotropy of inclusive $\mathbf{p}_t$ probe related to the vertex $\gamma(\mathbf{q},\mathbf{p}_t)$. If multiperipheral ladder of Fig.1 consists of scalar particles with triple coupling then a structure of inclusive vertex is determined in lowest order by Fig.2 where momentum $\mathbf{p}_t$ is fixed. Then the vertex can be written as 2-dimensional integral,

$$\gamma(\mathbf{q},\mathbf{p}_t) = g^2 \int d^2\mathbf{k}\, G(\mathbf{k})G(\mathbf{k} - \mathbf{p}_t)G(\mathbf{q} - \mathbf{k})G(\mathbf{q} - \mathbf{k} + \mathbf{p}_t), \tag{24}$$

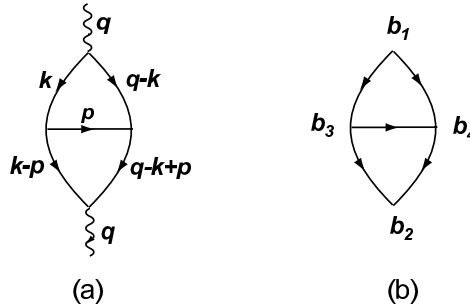where particle propagators G depend on 2-dimensional momenta only.

Figure 2: Simplest inclusive reggeon vertex

To estimate an anisotropy effect let us consider the vertex γ at small $q \sim p_t \ll \mu$ (here $\mu \sim r_0^{-1}$ is a typical mass parameter):

$$\gamma(p_t, q, z) \simeq \gamma(p_t^2)(1 - \epsilon \frac{q^2 p_t^2}{\mu^4} z^2 + \dots) , \tag{25}$$

where $z = \cos\phi$ is a cosine of the angle between $\mathbf{p}_t$ and $\mathbf{q}$. The coefficient which determines a degree of ellipticity is denoted as ϵ as we did before. For standard perturbative behavior of propagators: $G(\mathbf{k}) = (\mathbf{k}^2 + \mu^2)^{-1}$ numerical estimate gives a value $\epsilon \approx -0.2$ for scalar couplings g in the diagram 2. Note that such a sign corresponds to negative v_2 (in contrast to experimental observation).

The value and the sign of the effect depend on dynamical structure of the inclusive vertex $\gamma(\mathbf{q}, \mathbf{p}_t)$ – on form of propagators [1] and, more important, on structure of vertex of particle emission. Vertex properties are very sensitive to particle spin because it gives an extra azimuthal dependence. Calculations show that if inclusive particle has spin 1 , then the sign of ϵ is different (in accordance with data) and its value increases. Note that such situation is not far from reality because ρ-mesons give a considerable part of multiperipheral particles and pions due to their decays have mainly close transverse momenta. Numerical estimate gives $\epsilon \sim 0.5$.

Properties of the inclusive vertex $\gamma(\mathbf{q}, \mathbf{p}_t)$ can be studied experimentally in NN collisions, for instance by analysis of azimuthal two-particle correlations for hadrons in different windows of rapidity values.

Let us discuss behaviour of the inclusive vertex $\gamma(\mathbf{q}, \mathbf{p}_t)$ at large p_t. In region $\mathbf{p}_t^2 \gg \mu^2$ it should decrease according to perturbation theory in power-like way, $\sim (\mu/p_t)^m$, where a degree m depends on dynamics. In simple scalar theory (24) $\gamma(\mathbf{q}, \mathbf{p}_t) \sim (\mu/p_t)^4$, and z-depending coefficients decrease even faster, leading to a small ellipticity:

$$|\epsilon(p_t)| = \left| \frac{\gamma(q^2, p_t^2, z = 1) - \gamma(q^2, p_t^2, z = 0)}{\gamma(q^2, p_t^2, z = 1)} \right| \sim (\mu/p_t)^2 \quad \text{at } p_t^2 \gg \mu^2.$$

It means that a size of the p_t-probe becomes much smaller than μ^{-1} and its form becomes more isotropic.

The situation is different if the vertex includes particles with spin because in this case z-dependence of spin terms give an additional z dependence. As an example, in case of inclusive production of vector particles explicit calculation gives non-vanishing vertex ellipticity, $\epsilon(p_t) \to$ const when $p_t^2 \gg \mu^2$.

We discussed hitherto correlations of transverse momentum of the detected particle with respect to the reaction plane. The reaction plane orientation is difficult to reconstruct from experimental data, and often another method for studying anisotropic flow is used. It is related with analysis of two-particle azimuthal distributions, which contain an information on anisotropic flow. As it is seen from analysis of experimental data the main part of these correlations is related to the $\mathbf{p}_t - \mathbf{b}$ correlations for each particle. However, there are possible sources of two-particle correlations unrelated to the reaction plane, so called 'non-flow' correlations.

Corresponding two-particle inclusive reggeon diagrams are shown in Fig.3. To calculate anisotropic flows these diagrams should be estimated not at zero momentum transfer $\mathbf{q} = 0$ as for standard bi-inclusive cross section but at fixed value of impact parameter b.

The contribution of the diagram 3a is factorized in the impact parameter representation and contains factors corresponding to one-particle production of Fig.1b (see (23)).

$$F_{incl}^{(a)}(\mathbf{p}_t, \mathbf{k}_t; \mathbf{b}) \sim \left[T_{int}(b^2) + 4\epsilon(\mathbf{p}_t \cdot \mathbf{b})^2 T_{int}^{''}(b^2) \right] \left[T_{int}(b^2) + 4\epsilon(\mathbf{k}_t \cdot \mathbf{b})^2 T_{int}^{''}(b^2) \right] . \tag{26}$$

---

[1] Note that in case of Gaussian form of propagators, $G(k) = \exp(-k^2/\mu^2)$, the product of propagators in coordinate space does not depend on the angle resulting in zero anisotropy, $\epsilon = 0$.
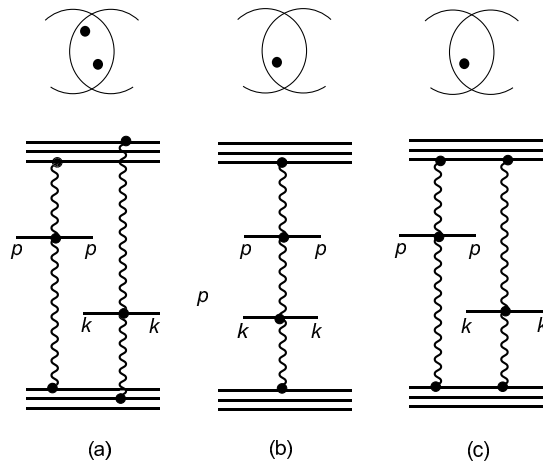
Figure 3: Reggeon diagrams for two particle inclusive production. (a) - particles p and k are emitted from different regions in transverse plane; (b) - p and k are emitted from a single reggeon chain; (c) - p and k are emitted from two reggeon chains attached to a single nucleon pair in colliding nuclei.

This results in factorized formula:

$$\left\langle e^{2i(\phi_{p_t}-\phi_{k_t})} \right\rangle = \frac{\int d^2\mathbf{p}_t d^2\mathbf{k}_t\, e^{2i(\phi_{p_t}-\phi_{k_t})}\, F_{incl}(\mathbf{p}_t,\mathbf{k}_t;\mathbf{b})}{\int d^2\mathbf{p}_t d^2\mathbf{k}_t\, F_{incl}(\mathbf{p}_t,\mathbf{k}_t;\mathbf{b})} = v_2(p_t)v_2(k_t)\ . \tag{27}$$

The contribution of diagram 3b is given by a convolution of T_{int} with two probes:

$$F_{incl}^{(b)}(\mathbf{p}_t,\mathbf{k}_t;\mathbf{b}) = \int d^2\mathbf{a}_1 d^2\mathbf{a}_2\, T_{int}(\mathbf{b}-\mathbf{a}_1-\mathbf{a}_2)\Gamma(\mathbf{a}_1;\mathbf{p}_t)\Gamma(\mathbf{a}_2;\mathbf{k}_t)\ . \tag{28}$$

This distribution (in the dipole approximation (22) with $\alpha = 0$) will contain higher derivatives of T_{int} over b^2:

$$F_{incl}^{(b)}(\mathbf{p}_t,\mathbf{k}_t;\mathbf{b}) \sim T_{int} + 8\epsilon^2(\mathbf{k}_t\cdot\mathbf{p}_t)^2 T_{int}'' + 32\epsilon^2(\mathbf{k}_t\cdot\mathbf{p}_t)(\mathbf{p}_t\cdot\mathbf{b})(\mathbf{k}_t\cdot\mathbf{b})T_{int}^{(3)} \tag{29}$$
$$+ 8\epsilon^2(\mathbf{p}_t\cdot\mathbf{b})^2(\mathbf{k}_t\cdot\mathbf{b})^2 T_{int}^{(4)}\ .$$

All ϵ^2-terms are at $b \sim R$ of the same order of value, $O(1)$, and are small compared to the main term in Eq.(26), which is of order $O(R^2) \sim A^{4/3}$. So extra unfactorized correction to Eq.(27) due to diagram 3b is inessential.

The situation is different for diagram 3c. Its isotropic part has a smallness of order $A^{-4/3}$ in comparison with isotropic part of $F_{incl}^{(a)}$. The anisotropic part contains a 'non-flow' term $(\mathbf{p}_t\cdot\mathbf{k}_t)^2$ which contains the overlap function T_{AB} (not its derivatives). As a result its contribution to (27) is of the same order as due to factorized structure $(\mathbf{p}_t\mathbf{b})^2(\mathbf{k}_t\mathbf{b})^2$ from Eq.(26). This contribution violates factorization in Eq.(27) for two-particle correlation. Note that the 'flow' and 'non-flow' structures have different dependence on impact parameter.

Now we will try to estimate contributions to azimuthal asymmetry coming from multi-pomeron interactions. The simplest reggeon diagram of Fig.1b gives main contribution to inclusive cross section. Contributions of multipomeron diagrams of Glauber type cancel each other because of the AGK rules [10].

In reggeon theory with $\alpha_P(0) > 1$ the number of pomeron exchanges increases with energy, so a role of inter-pomeron interactions grows. Detailed analysis of multipomeron effects will be published in other publication, and here we will discuss briefly physical reasons for possible increase of azimuthal anisotropy.

When energy increases a longitudinal length of the nucleon tube with fixed transverse position is contracted and multiperipheral fluctuations connected to each of fast nucleons overlap each other in longitudinal size. Therefore a probability for particles (partons) of different chains (related to different nucleons) to interact increases. Two chains can either fuse to a single chain (triple pomeron interaction) or rescatter without changing a whole chain number (2-2 or, more generally, n-n pomeron vertices). Effects of fusion become noticeable already at RHIC energies,

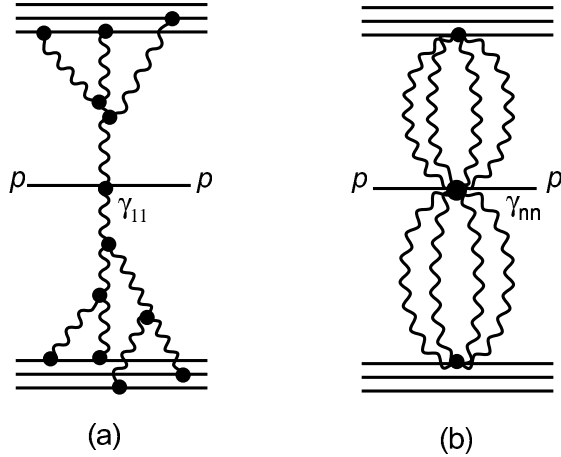(a)   (b)

Figure 4: Multipomeron diagrams for inclusive production: (a) - diagrams with fusion and splitting of parton chains; (b) - diagrams with rescattering of n parton chains.

resulting in reduction of secondary density about two times as compared with the eikonal approximation [11]. This effect is mainly due to diagrams with three-pomeron interaction (Fig. 4a). But due to their sign-alternating character a profile of the amplitude becomes more smooth and the azimuthal asymmetry becomes even smaller because of smaller gradients of parton density.

Different situation is realized for diagrams with chain rescattering (Fig. 4b) which give positive contributions to inclusive cross section. Even if the total inclusive cross section changes slightly due to such rescatterings, its anisotropic part may be strongly increased. Indeed, the expression (18) for inclusive cross section will contain in case of n interacting chains a convolution $T_A^n \otimes T_B^n$ instead of $T_A \otimes T_B$. Azimuthal asymmetry is determined by density derivatives (see (21)), therefore an extra factor $\langle n(b) \rangle^2$ will appear in expression for v_2. The number of interacting pomerons at RHIC energies is not large ($\langle n(b) \rangle \sim 2$ for central collision), but increase of v_2 can be considerable because the effect is quadratic in n. Note that $\langle n(b) \rangle$ increases with atomic number A and changes the A dependence for v_2 also. The same mechanism may give an increase of $\langle p_t^2 \rangle$.

Let us present examples of numerical estimates of elliptic flow for the exponential parametrization (6) of the inclusive vertex. They are illustrative only. We intentionally do not fit experimental data because, first, little quantitative information on the inclusive vertex γ exists and, second, it is necessary to have more reliable model for nuclear multipomeron effects. We aim to demonstrate that qualitative features of elliptic and directed flows peculiar to the mechanism under discussion are in agreement with experimental observations. In particular, as it is seen from Eq. (21) the value of $v_2(p_t, b)$ grows with increase of both transverse momentum p_t and impact parameter b.

Fig.5 presents the b-dependence of elliptic flow. According to Eq. (21) v_2 grows as b^2 (thick solid line, $\epsilon = 0.4$) in contradiction with the experimental behavior at very large b when nuclei only touch each other. Let us note here that in the case of very large impact parameter values where nuclear densities are quite small an accuracy of the model is low. This is why calculation results for $b > 8$ fm are shown with dotted curves. The dashed curve corresponds to the simplest
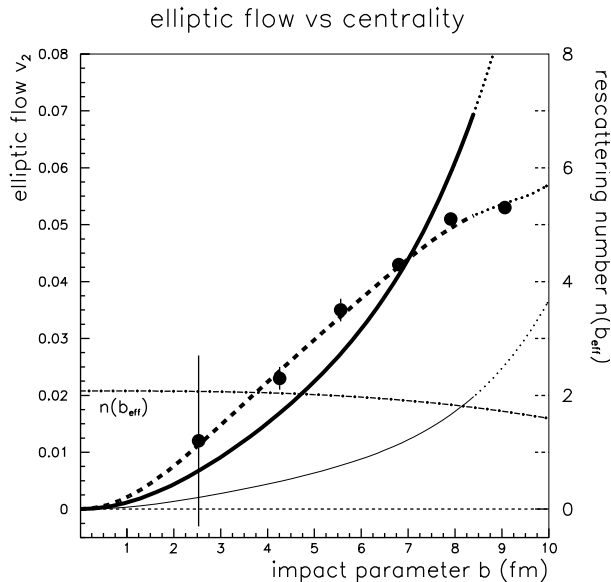
Figure 5: Elliptic flow v_2 as a function of impact parameter b at $p_t = 0.5$ GeV/c. Calculations for $b > 8$ fm are shown with dotted curve. Thick solid line corresponds to calculations at $\epsilon = 0.4$. Thin solid line corresponds to calculations at $\epsilon = 0.1$, and dotted line – at $\epsilon = 0.1$ multiplied to the mean rescattering number squared $n(b_{eff}) = n(0.65\,b)$. The dashdotted line at this picture gives $n(b_{eff})$ as a function of b (the right scale).

account of nuclear effects due to inter-pomeron interactions – calculations at smaller parameter value $\epsilon = 0.1$ (thin solid line) are multiplied to the factor $n(b_{eff})^2$. The function $n(b_{eff})$ gives an effective number of interacting pomeron fluctuations [2]. It is also presented at the figure (dash-dotted line) and one can see that the maximal number of pomeron interaction is about 2 for central collisions. Experimental data are from [12].

Our main aim is to draw attention to the mechanism of appearance of azimuthal correlations between produced particles related to specific parton correlations in initial states of colliding nuclei, and which is not caused by particle interactions in the final state.

The mechanism under discussion is connected with correlation between partons transverse momenta and the gradients of density of surrounding (parent) partons. This can lead to correlation between parton transverse momentum and its transverse position inside nucleus. As a result transverse momenta of partons in incoming nuclei (before collision) are already partially aligned along transverse nuclear radiuses. The non-central collision of nuclei selects the asymmetric overlapping part of the fast nucleus resulting in $\mathbf{p}_t - \mathbf{b}$ correlations for produced particles.

We discussed this phenomena using the simplest reggeon diagram in order to emphasize the fact of its existence. For quantitative description of asymmetries it is necessary to account for a more complicated mechanism related to interactions between different chains. We emphasized that this mechanism can substantially increase elliptic flow and modify its atomic number dependence. Role of multipomeron interactions describing these effects increases with energy and is important at RHIC energies. This mechanism influences dependence of asymmetries on centrality, transverse momenta and rapidity.

Evidently the final state interaction can also contribute to azimuthal asymmetry of produced particles. In order to obtain an information on properties of hadronic matter at high temper-

---

[2]   The function $n(b)$ was estimated in the eikonal approximation with effective parton-nucleon cross section value $\sigma \sim 10$ mb. The mean position of interacting nucleon in a nucleus was taken as $b_{eff} = 0.65\,b$.

atures and densities it is crucial to separate effects due to initial and final state interactions. In particular it is important to carry out a detailed investigation of azimuthal correlations of particles produced in nucleon-nucleon and nucleon-nucleus interactions. Such studies will be possible in high-multiplicity events at LHC.

References

[1] K.G. Boreskov, A.B. Kaidalov, O.V. Kancheli, Sov. J. Nucl. Phys. **74** (2009).

[2] J.-Y. Ollitrault, Phys. Rev. D **46**, 229 (1992).

[3] J.-Y. Ollitrault, Phys. Rev. D **48**, 1132 (1993).

[4] S. Voloshin, Y. Zhang, Z. Phys. C **70** (1996) 665.

[5] H. Sorge, Phys. Rev. Lett. **78**, 2309 (1997).

[6] S.A. Voloshin, Nuclear Physics A, **715**, 379 (2003).

[7] S. S. Adler *et al.*, PHENIX Collaboration, Phys. Rev. Lett. **91**,182301 (2003).

[8] M. Tonjes (for the PHOBOS Collaboration), J. Phys. G. **30**, S1225 (2004).

[9] J. Adams *et al.*, STAR Collaboration, Phys. Rev.C **72**, 014904 (2005).

[10] V.A. Abramovsky, V.N. Gribov, O.V. Kancheli, Yad. Fiz. **18**, 595 (1973), Sov. J. Nucl. Phys. **18**, 308 (1974).

[11] A.B. Kaidalov, Phys. Usp. **46**, 1121 (2003), Usp. Fiz. Nauk **46**, 1153 (2003).

[12] STAR collaboration, Phys. Rev. C **66**, 034904 (2002).